

c2



# Lawrence Berkeley Laboratory

UNIVERSITY OF CALIFORNIA

## Accelerator & Fusion Research Division

Submitted to Review of Scientific Instruments

Development Testing of the U.S. Common Long  
Pulse Source at 120 kV

M.C. Vella, W.S. Cooper, P.A. Pincosy,  
R.V. Pyle, P.D. Weber, and R.P. Wells

December 1987

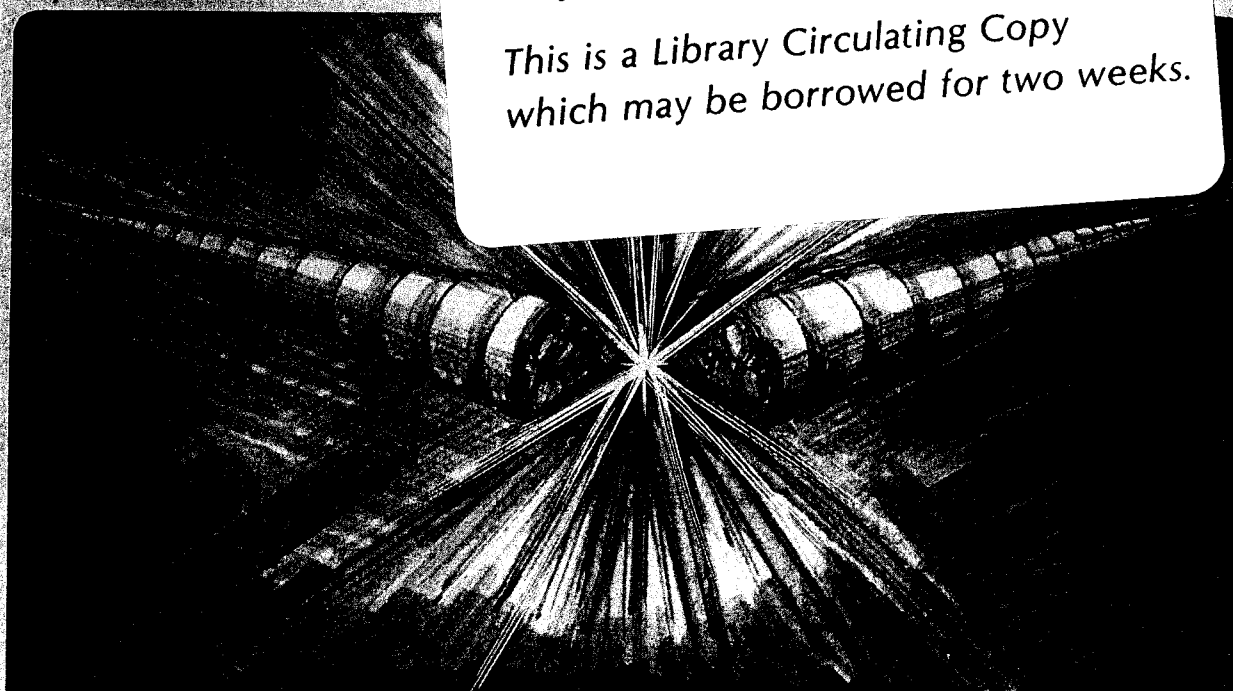
RECEIVED  
LAWRENCE  
BERKELEY LABORATORY

SEP 30 1988

LIBRARY AND  
DOCUMENTS SECTION

**TWO-WEEK LOAN COPY**

*This is a Library Circulating Copy  
which may be borrowed for two weeks.*



LBL-22530  
c2

DISCLAIMER

This document was prepared as an account of work sponsored by the United States Government. Neither the United States Government nor any agency thereof, nor the Regents of the University of California, nor any of their employees, makes any warranty, express or implied, or assumes any responsibility for the accuracy or completeness of the information contained herein.

c.2

LBL-22530

**Lawrence Berkeley Laboratory Library**  
University of California, Berkeley

## Development Testing of the U.S. Common Long Pulse Source at 120 kV

M.C. Vella, W.S. Cooper, P.A. Pincosy<sup>a)</sup>, R. V. Pyle, P.D. Weber<sup>b)</sup>, and R. P. Wells

Lawrence Berkeley Laboratory, University of California, Berkeley, California 94720

The U.S. magnetic fusion energy program has developed a single design long pulse neutral beam source for TFTR, MFTF-B, and DIII-D. The arc is a very compact axial magnetic line cusp. The accelerator is an actively cooled tetrode with water cooled grid tubes of shaped molybdenum forming "slot" beamlets. DIII-D and MFTF-B configurations have an 80 kV accelerator gap, with 12 x 48 cm aperture, and a 10 meter "module" focus. TFTR modules are unfocused, with a 120 kV gap and 12 x 43 cm mask.

The first CLPS was tested in the TFTR configuration, at 120 kV, 2 seconds. Optimum current was 73 Amperes, or 1.76  $\mu$ pervs (deuterium), with 80% - 85% atomic fraction. Optimum divergence of ions plus neutrals was 0.4° parallel to the slots, and 0.7° perpendicular to the slots (1/e half angle). The combination of an axial cusp magnetic bucket and slot accelerator apertures gives the CLPS about twice the beam power per unit cross section of other long pulse sources, plus lower divergence in the direction parallel to the slots.

## Introduction

The U.S. magnetic fusion energy program has developed a long pulse positive ion neutral beam injector, called the Common Long Pulse Source (CLPS), for the Princeton TFTR tokamak, Livermore MFTF-B tandem mirror, and GA Technologies (GAT) DIII-D tokamak. As summarized in TABLE 1, the CLPS was intended to operate deuterium or hydrogen in three accelerator configurations: (1.) 12 cm x 43 cm aperture, 120 kV gap, unfocused (TFTR); (2.) 12 cm x 48 cm aperture, 80 kV gap, unfocused (MFTF-B); and (3.) 12 cm x 48 cm aperture, 80 kV gap, focused (MFTF-B and DIII-D). All versions share the same plasma generator, accelerator grid modules and insulator stack.<sup>1</sup> The major components are illustrated in an assembly drawing shown in Fig. 1. If the full 12 x 48 cm aperture were used, a 120 kV CLPS would be capable of 80 Amps of deuterium, or 115 Amps of hydrogen.

Long pulse neutral beam source development began at LBL in 1978.<sup>2</sup> Long pulse heating beams have also been developed for the JT-60 tokamak in Japan,<sup>3</sup> for the Joint European Torus (JET),<sup>4,5</sup> and by the Oak Ridge National Laboratory (ORNL).<sup>6</sup> All have electrostatic accel-decel tetrode accelerators. The performance and space requirements of the U.S. users correspond to approximately a factor of two increase in beam power per unit source cross section, which dictated unique approaches to plasma generator and accelerator design. This paper was written to summarize the most important CLPS features for the magnetic fusion research community.

U.S. development was strongly motivated by an MFTF-B requirement for 80 kV, 30 second positive ion based neutral beams. Development sources were built and tested by ORNL and LBL. The LBL prototype had a 10 x 40 cm accelerator, which, like the CLPS was essentially a cw design.

Pulse length specifications for TFTR and DIII-D were dictated by temperature limits on each user's inertially cooled ion dumps. Delay of MFTF-B eliminated the need for 80 kV, unfocused units, since existing sources could be reconfigured later.

The essential CLPS performance requirement was for 70 Amps of deuterium at 120 kV from the 12 x 43 cm TFTR configuration, with 80% atomic fraction. Commonality restricted the space envelope to the minimum set of user enclosure dimensions: 42 x 86 x 80 cm. The 42 x 86 cm cross section is for TFTR, and the 80 cm depth for DIII-D. Aperture areas and focal length were set by the limiting user beamline apertures.

The CLPS baseline design began by extending the 10 x 40 cm long pulse prototype to 12 x 48 cm, within the same space envelope. The 10 x 40 cm source had delivered 54 Amperes of deuterium at 120 kV<sup>7</sup>, and 56 Amps of hydrogen at 80 kV.<sup>8</sup> This extrapolated to 70 Amperes deuterium at 120 kV with 12 x 43 cm TFTR mask, and to 80 Amperes hydrogen at 80 kV with the 12 x 48 cm mask.

The major technical challenge of the CLPS was the uniformity and operability of the plasma generator. The critical engineering aspects of the source are dissipation of beam heat on the grids, and of backstreaming electron power on the arc backplate. Testing of the 12 x 43 cm, 120 kV TFTR version was technically appropriate, since it has 40% more beam power than the 12 x 48 cm, 80 kV hydrogen configuration. The procurement schedule gave priority to delivery of TFTR sources and was success oriented (i.e., high risk), since production had to begin before completion of the first beam tests. Risk was mitigated by early assembly of two sources for testing. Development modifications were incorporated into downstream production, and retrofit on early units.

Focusing was required for the DIII-D and MFTF-B versions because the accelerator aperture was larger than minimum beamline apertures. The beam footprint was reduced by inclining the outer pair of the four (flat) accelerator modules, i.e., modular focusing. Simulations indicated acceptable beamlet optics at the module interfaces.<sup>1</sup>

Testing was carried out at LBL on the Neutral Beam Engineering Test Facility (NBETF). Development of the arc for 12 x 48 cm hydrogen operation was completed after beam testing, on an arc test stand (Test Stand IIA). The first beam operation with hydrogen was on the TFTR test stand.<sup>9</sup> First beam operation with production arc filaments was on the TFTR and DIII-D heating beamlines.<sup>10,11</sup> DIII-D operation also constituted the first test of the 12 x 48 cm aperture, and of modular grid focus.

The CLPS procurement was supported jointly by TFTR and DIII-D, and managed by the Lawrence Livermore National Laboratory. The contract was won by the New Products Division of RCA (Lancaster, PA), which adapted the baseline design for production and constructed 24 sources — 15 configured for TFTR, and 9 for DIII-D. Two TFTR units were tested at LBL. The first production accelerator was tested to 120 kV, 2 seconds, and the third production accelerator was run briefly to check its conditioning rate.

#### **I. The Neutral Beam Engineering Test Facility (NBETF)**

Beam testing was done on the LBL Neutral Beam Engineering Test Facility (NBETF), which had previously been used for the 80 kV, 30 second and 120 kV, 2 second tests of the 10 x 40 cm LBL prototype, and for the 80 kV, 30 second test of the 12 x 43 cm ORNL prototype.<sup>6,7,8</sup> The main injector tank was cryopumped, and identical to the TFTR beamlines. The

high voltage supply was an unregulated transformer-rectifier with SCR switching, rated at 130 kV, 80 Amperes.<sup>12</sup>

Source electrical waveforms were displayed in both analog and digital form. In addition to the usual arc and beam volt-amp data, the floating potential of the first grid, probe plate, and filament floating plates were monitored. Computerized source, beamline, and target waterflow calorimetry was also available.

Beam divergence data were obtained from: (1.) The Optical Multichannel Analyzer (OMA), a Doppler shifted spectral diagnostic; (2.) Short pulse, inertial calorimeter; and (3.) Long pulse beam target. The OMA spectral diagnostic has been used routinely for years.<sup>13</sup> Line emission from excited beam neutrals was observed through windows in a box between the accelerator exit and the neutralizer. The Doppler shifted lines provide information about beam energy, divergence, species, and impurities. By convention, the species mix of positive ion neutral beams is referenced to the plasma generator. The OMA species is inferred from the intensity of Doppler shifted Balmer alpha lines of full, half, and third energy neutrals, assuming equilibrium neutralizer thickness. Divergences of the three beam components are obtained from the widths of the peaks. The only impurity tracked was water, which was  $\leq 0.2\%$ .

Due to instrumental noise, good background subtraction is critical to the OMA. Background data were taken during arc only shots, with arc power and arc voltage similar to a beam shot. A poor background is evidenced by poor baselines in the spectra, and affects the relative peak heights of the species. With good baselines, the OMA gave  $\pm 2\%$  species reproducibility, and agreed with results from the low energy magnetic momentum analyzer on Test Stand IIA.

Since the ion separation magnet had been removed for long pulse testing, neutralizer thickness was insured by operating with gas flows near 17 TI/s, which had given equilibrium thickness during half second testing with a magnet. Also, data were taken over a range of gas flows, 14 to 24 TI/s, with similar species and perveance results.

The short pulse, inertial calorimeter was downstream of the cryopumped tank, 9.9m from the accelerator. It consisted of two plates, arranged in a "vee", with an array of 17 x 9 thermocouples arranged. The halves of the "vee" were retracted for long pulse shots.

The long pulse target was in a separate vacuum tank. Active target cooling was based on a 1,500 hp, 200 psi, 5,000 gpm water system, with an 11,400 gallon reservoir, cooled by heat exchangers and local evaporation towers. The target calorimeter had to dissipate both ion and neutral beam power, up to 8.9 MWatts.

The active target<sup>14</sup> had eight panels, arranged in a "vee" with four panels on a side. The apex was about 11.5m from the exit aperture of the accelerator. The panels were individually positioned and rotated. Each panel had five nesting subpanels, mounted on a pair of water manifolds. Each subpanel had an inlet and outlet thermocouple, giving a five by eight array. The main target manifolds, and the manifolds for the eight panels, also had thermocouple pairs for overall calorimetry checks.

The NBETF test stand shared the building with the LBL 184 inch cyclotron. Stray magnetic fields of 2 to 3 Gauss from the cyclotron caused separation of beam ions and neutrals over the 11 meters from the accelerator to the calorimeter. Correction coils were installed around the cryo-pumped injector tank to minimize the ion separation. The stray fields were vertical, i.e., in the 48 cm direction. The resulting ion drift



was parallel to the accelerator slots, which increased the parallel beam divergence measured by the calorimeters.

After initial accelerator conditioning, testing was paced by repair of leaks in the water bellows on the subpanel manifolds. The probable cause of the bellows failures was over-compression, due to excessive panel flexing associated with unexpectedly high power densities. The subpanels had been designed for  $\leq 2$  kWatts per square centimeter. The angle and spacing of each panel arm were adjusted to spread the beam power over as many subpanels as possible. However, the beam current was higher, and the divergence lower, than expected. Center subpanels routinely exceeded 2.2 kW/cm<sup>2</sup>, and the maximum power density exceeded 2.8 kW/cm<sup>2</sup>.

The accelerator and plasma generator had a separate water cooling system, 100 gpm at 300 psi. Resistive high voltage power drain through the water lines was minimized by keeping source cooling water at 1 — 2 M $\Omega$ -cm. To prevent oxidation of the molybdenum grid tubes and plasma source mask, the oxygen content of the source water was maintained below 80 ppb. Arc coolant was shared between major components, but the backplate was monitored separately, because it dissipated most of the backstreaming electron power.

## **II. Accelerator Background**

The first LBL long pulse prototype had a 10 x 10 cm accelerator aperture, masked to 7 x 10 cm, with a field-free plasma generator (i.e., no external magnets). Like the CLPS, the electrostatic accelerator was an accel-decel tetrode, with slot beamlets formed by hollow molybdenum grid tubes.<sup>2,15</sup>

The 7 x 10 cm source reached 4.8 seconds at 120 kV, and 28 seconds

at 80 kV. It was relatively difficult to operate, probably due to the high gas flows and varying plasma uniformity of the field-free plasma generator.<sup>16</sup> Small magnetic bucket plasma sources were also tried, with arc and low frequency inductive rf power.<sup>17,18</sup> These bucket sources had poor plasma uniformity, due to the magnet layout, but had higher gas efficiency and atomic fraction than the field-free source.

The 10 x 40 cm long pulse accelerator, with a magnetic bucket plasma generator, was built next.<sup>19</sup> It had four flat grid modules per electrode, similar to the CLPS.<sup>1,20</sup> All three accelerator generations used the same grid shapes and gaps, which suggests that the evolutionary reduction in beam divergence and improved operability are due to improvements in the plasma generator.

CLPS accelerators have a 12 x 48 cm tetrode grid structure, with four identical modules per electrode. The accelerator aperture is defined by a mask, either 12 x 43 cm, or 12 x 48 cm. The 43 cm version has 45 beamlet slots, and the 48 cm has 55 slots. Each module is a brazed assembly, with fourteen grid tubes per module. "Focusing" is accomplished by inclining the outer pair of the four modules ( $1.08^\circ$  for 10 meter focus). Electrode gaps and module focus are set by alignment shims.

The 14 shaped molybdenum grid tubes in each module are brazed to hollow stainless steel "fingers",<sup>21</sup> which carry water from the module base to each grid tube. The fingers hold each tube in slight compression, and provide thermal stress relief. The modules are mounted on a grid holder, and aligned with shims to form each grid electrode.

Module alignment begins with the straightness of each tube, and is fixed during brazing. In production, brazing of the grid modules became routine. On the other hand, procurement of grid tubes paced production,

especially the relatively long source and gradient grid tubes. The source grid tube is diamond shaped, 18 cm in length, 0.36 cm wide by 0.28 cm high, and straight to  $\pm 0.003$  cm.

The accelerator corona rings are gun drilled stainless steel and double as water manifolds. Each grid is cooled in halves, i.e., the modules are paired on a manifold for one half of each grid, with inlet and outlet hoses for each half. Water for the plasma and gradient grids (grids 1 and 2) is brought from ground to high voltage. Since hose length was limited by the enclosure, maximum hose diameter was dictated by high voltage power drain. Water for the suppressor and ground grids (grids 3 and 4) is brought from ground.

To minimize neutralizer plasma leakage onto the suppressor grid and backstreaming electron leakage through the structure, the gap between the fingers was a nominal ten mils. To accommodate focusing, a relatively large gap (approximately 0.3 cm) was left between neighboring modules. On the fourth (ground) grid, overlap tabs on the ends of the modules cover these gaps between modules, to prevent particle leakage from the neutralizer plasma onto the suppressor.

Overlapping tabs were not provided for the gaps between the modules of the suppressor and gradient grids. The assumption (apparently mistaken) was that blocking gaps on the grid 4 (ground) modules would be sufficient to eliminate significant back electron transport through the gaps between the modules of grids 1-2, and 2-3. During beam testing, darkening was observed on the plasma grid half of the insulator between the first and second grids, opposite the module gaps. This may have been due to a line of sight for secondary electrons from the suppressor grid, through the gradient grid modules to the insulator. These dark lines had

no observable effect on operation.

The most obvious difference between the 10 x 40 cm and CLPS accelerators is replacement of a brazed ceramic insulator stack with epoxy. Epoxy is inexpensive and easily repairable, but outgasses during initial conditioning. The choice of epoxy was dictated by cost. The estimated added cost of a brazed insulator stack was \$150k to \$200k per source. The delivered CLPS cost was about \$550k per assembled source (plasma generator and accelerator), including four water cooled quarter inch OD plasma probes.

The first accelerator (A1) was run with the first two plasma generators (P1 and P2) for the 120 kV testing reported here. Accelerator A2 was tested on the TFTR test stand, with plasma generator P3. The first true production accelerator, A3, was also shipped to LBL with plasma generator P4, to check the conditioning rate.

### **III. Plasma Generator Background and Development**

The principal technical challenge was to obtain a uniform and reliable hydrogen plasma over the 12 x 48 cm extraction area. Reliability requires a low frequency of short shots due to arc spots, plus operability (i.e., freedom from instabilities). The development philosophy was to seek acceptable plasma uniformity ( $\leq 15\%$  max/min) over the widest operating window of gas flow, arc power, and arc voltage. Best data were routinely ignored. Approximately ten magnet arrangements and forty filament combinations were tried in arriving at the production setup. Arc development was carried out on Test Stand IIA, with an array of twenty button probes, biased -20 Volts with respect to cathode to measure saturated ion current density. The ion species mix was measured with a

low energy magnetic momentum analyzer.

High current neutral beam sources began in the 1970's with field-free arc chambers, which powered 2XII-B, TMX, TFTR, and DIII. Field-free arcs had multiple filaments, and no external magnetic field.<sup>22</sup> The atomic fraction was only 55% - 65% (hydrogen or deuterium). Magnetic arc chambers developed later at ORNL, JET, and JAERI had higher atomic fraction, plus higher gas and power efficiencies.

The magnetic bucket of the 10 x 40 cm prototype was intended to produce 80% atomic fraction. JET and JAERI had used azimuthal multi-cusp designs, which require a relatively large distance from the sidewall magnets to the edge of the extraction area. Since TFTR had limited sidewall space, LBL chose an axial multi-cusp design (i.e., bucket cusps parallel to the beam direction) for both the 10 x 40, and CLPS. Axial geometry is very compact, and the CLPS has only 6 cm from the projection of the extraction edge to the sidewall. Like JET and JAERI, the CLPS has multiple filaments, but wired in parallel across picture frame plates. The plates and bucket are made of OFHC copper.

As part of the 10 x 40 program, a low frequency, inductively coupled rf plasma generator was also developed.<sup>17,18</sup> The goal was long lived plasma generator technology. Performance was slightly better than with an arc in the same buckets, but rf was dropped to maintain compatibility with the existing user dc power supplies.

The CLPS arc began as a geometric scaleup (i.e., ratio 12x48:10x40) of the number of filaments and backplate magnets on the 10 x 40. Arc spots were minimized by designing the cathode assembly plates with overlapping edges, and plating the plasma sides of the copper plates with a few mils of dull nickel. The nickel plate was inexpensive, and proved

resistant to sputter damage. Outgassing in the poorly pumped gaps between the filament plates makes initial arc conditioning critical. Minimal damage and long arc life are best assured if initial conditioning is at the lowest possible gas flow (dependent on outgassing) during the first few hours of arc operation.

Compared with the 10 x 40, the CLPS bucket has improved: (1.) Magnetic bucket symmetry; (2.) Net backplate flux; and (3.) Filament design. The number of axial line cusps was increased from 36 to 40, to give net zero bucket flux in each quadrant (i.e., quadratic symmetry). Reasonable uniformity was first obtained by adjusting the net magnetic flux of the backplate to obtain a field-free area ( $0 \pm 0.2$  Gauss) over 12 x 48 cm at the front flange of the bucket.

The 10 x 40 cm arc had 0.152 cm (0.06 inch) diameter tungsten filaments, with a hairpin shape that was doubled over on itself. The CLPS began with this design, which offered adequate cathode without intruding into the projection of the extraction area. The 10 x 40 cm arc had marginal plasma uniformity with deuterium, and was susceptible to plasma instabilities, called mode flips.<sup>23</sup> Hydrogen could only be run by resistively tying the probe plate to the bucket wall, to add anode area. This proved impossible with the CLPS — even 50 Amps to the probe plate destroyed uniformity over the larger extraction area.

Arc development was greatly influenced by a visit of JAERI staff.<sup>24</sup> Based on experiment<sup>25</sup> and simulation,<sup>26</sup> JAERI believed that arc uniformity, species, efficiency, and stability could be simultaneously optimized by the relationship of the filaments and magnetic fields. Once the backplate magnet setup had been found, performance was optimized by positioning the filament tips in the magnetic field.

By the end of the initial beam testing period (Ref. Section IV), the first JAERI inspired filament design (designated J1) had demonstrated better operability and efficiency on the arc test stand than the hairpins. Profile and species were similar. Plasma chamber P1 with 32 of the J1 filaments (P1-32J1) was used on NBETF to complete 120 kV, 2 second beam testing. The two filament types are shown in Fig. 2. All filament shapes had the same wire length to allow operation with mixed shapes, electrically in parallel across the filament heater supply.

Subsequent to the test reported here, arc development continued on Test Stand IIA to obtain a uniform hydrogen plasma over the 12 x 48 cm aperture. The filament setup specified for production uses 32 filaments: 24 type J6; 4 type J3; and 4 type J8. Compared with the J1's, production filaments have three different heights, different planes of the emitting bend, and offsets of the bend relative to the legs. With J-filaments, the arc demonstrated: 15% maximum/minimum hydrogen ion uniformity over the 12 x 48 cm accelerator area; 83 - 85% atomic fraction; and stable operation with both deuterium and hydrogen.

All of the J-filament shapes gave higher power efficiency than the hairpins. The arc power required for 230 mA/cm<sup>2</sup> deuterium was reduced to 100 kWatts (from 150 kWatts with 44 hairpins). With the TFTR aperture, 230 mA/cm<sup>2</sup> corresponds to  $12 \times 43 \times 0.6$  (transparency)  $\times 0.230 = 71.2$  Amperes extracted, or, 0.71 Amps per kWatt of arc power. (The 44 hairpins gave 0.47 Amps per kWatt.) A more representative efficiency measure, based on the 12 x 48 cm<sup>2</sup> extractable area, is 0.79 Amps per kWatt.

Arc chambers P1,2,3 began with stainless steel flanges brazed to a copper bucket. The stainless steel was damaged by arc spots to adjoining

plates (the probe plate and the forward spacer of the filament sandwich), and units P4-24 were given copper flanges. The copper flanges resulted in marginal structural rigidity (i.e., both ends of the bucket must be bolted to a stiff plate before pump down), but eliminated spotting damage. Buckets P1,2,3 were later retrofit with copper flanges.

The first beam operation with production filaments actually took place on the TFTR and D-III heating beamlines, where they have worked very well.<sup>10,11</sup>

#### IV. Initial Accelerator Testing

On arrival, accelerator A1 was observed to have gaps approximately  $\leq 0.2 \text{ cm}^2$  between the four modules of the fourth grid (six gaps, three per side). These were covered in production units by reducing the inner dimension of the fourth grid alignment shim, but initial accelerator testing began as-delivered, because other design and tolerance oversights which were also apparent. Initial high voltage conditioning of A1 was extremely slow, and improved only when these gaps were covered with hand fit molybdenum tabs. Vertical gaps between the plasma source grid and mask were also noted. In retrospect, the gaps between the modules of the fourth grid were critical, but gaps between the plasma grid mask and grid was less so — A1 reached full power with this flawed mask.

Based on infrared analysis and x-ray photoelectron spectroscopy, RCA identified a problem with surface contaminants.<sup>27</sup> To insure safe storage and handling, the accelerator components had been stored in anti-static plastic bags, in a clean room. Using control samples, plasticizer from the anti-static bags was identified as the principal surface contaminant. Contaminants from vinyl gloves and texwipes were also identified.



Revised handling procedures specified glass or untreated polyethylene containers, and latex gloves. Washing solvents left insignificant residues.

Beam operation on NBETF began with 44 hairpin filaments, in source unit designated A1/P1-44H. After three months, the accelerator fault protection was allowing an average of 0.5 msec per beam try at 40 kV. By the end of February, this had improved to only 2 - 3 msec per try. Source P2-44H was also tried, with little improvement.

The gaps between the modules of the fourth grid were then covered with hand-fitted molybdenum tabs, with immediate improvement in the conditioning rate. With up to ten interrupts per shot, A1/P2-44H reached 95 kV, 2 seconds in two weeks. A possible explanation is that ions from the neutralizer plasma had been leaking through the gaps between the modules of the ground grid, generating secondary electrons on non-beam carrying areas of the suppressor structure. Since the other grids lacked overlapping tabs between modules, secondary electrons could cascade back through gaps between modules, causing high voltage breakdown.

Testing with A1/P2-44H was halted at 115 kV, 1 second by failure of a main bearing on the 1,500 target water pump. During pump repair, arc P1-32J1 was mounted on NBETF, marking the end of the initial accelerator test period.

## **V. 12 x 43 cm, 120 kV CLPS Beam Properties**

Plasma generator P1-32J1 was used because it had demonstrated excellent operability on the arc test stand. Plasma uniformity was insensitive to changes in arc voltage between 75 and 100 volts, and to changes in gas flow between 14 and 20 TI/s. With hairpin filaments, plasma uniformity had been sensitive to  $\pm 0.25$  Gauss of external magnetic

field. However, P1-32J1 could tolerate  $\pm 1.5$  Gauss (three axes), and was operable with both hydrogen and deuterium.

A wide 90 kV perveance tune, illustrated in Fig. 3, was taken to obtain extensive calorimetric data. Since only the main beam target was capable of high heat flux dissipation ( $\geq 1$  kW/cm<sup>2</sup>), the intention was to restrict the perveance range above 90 kV to protect the beamline. The gradient grid bias was 14% of accel voltage, and the gas flow was 14 to 24 TI/s. The data scatter below 0.8° perpendicular divergence is due to difficulty resolving small divergences, since most of the power was on only six subpanels.

Source A1/P1-32J1 reached 120 kV, 2 seconds in a few days — paced by repair of target water leaks, rather than accelerator conditioning. Over one hundred two-second shots were accumulated in another four days of operation, also paced by target leaks. At 120 kV, optimum current was 71 to 73 Amperes deuterium, or, 1.70 to 1.75  $\mu$ pervs. Beam divergences (1/e half angle) were  $\leq 0.4^\circ$  parallel to the slots, and  $\approx 0.7^\circ$  perpendicular to the slots (ions plus neutrals). Requested beam time was usually 2.4 seconds, to ensure two seconds on the occasional shot which reached the maximum number of interrupts. Interrupts were 8 msec duration. The number of interrupts per shot fell from 10 to about 2 by the end of the run. The average shot was 2.3 seconds,  $\pm 6\%$ . The shortest shot was 2.0 seconds, and the longest, 2.5 seconds. The OMA indicated 80 to 85% atomic deuterium ions at the plasma source.

Attempts to operate near optimum perveance at 120 kV were terminated by target water leaks. The decision was made to operate underdense (i.e., below optimum perveance) for the remainder of the hundred shot test, to preserve the target. This reduced the power density

on target by lowering the beam current and increasing the divergence.

To operate underdense, the gradient grid bias was first reduced to 12.7%, but reliability was poor. Most of the hundred shots were at 13.2%. The one hundred, 120 kV, 2 second shots averaged 121.3 kV (standard deviation,  $\pm 1\%$ ), 68.1 Amps ( $\pm 2.7\%$ ) and 1.6  $\mu$ pervs ( $\pm 3.4\%$ ). Maximum voltage was 123.8 kV, and minimum was 119.5 kV. The current range was 64.5 to 73.2 amperes (deuterium), or, 1.5 to 1.8  $\mu$ pervs.

Selected 120 kV, 2 second divergence data are plotted in Fig. 4, which illustrates that the attempt to restrict the perveance range over a hundred shots had qualified success. Most shots were in a very narrow perveance range, but the overall range was similar to the 90 kV tune. The lower optimum perpendicular divergence at 120 kV reflects the diminished importance of ion thermal energy. The  $0.4^\circ$  divergence parallel to the slots was obtained during a cyclotron shutdown with minimal residual magnetic field. The OMA consistently indicated a smaller total beam divergence than the calorimeters, as expected, since OMA data were taken a meter from the accelerator. On average, 85% of the accelerator power was observed calorimetrically at the target.

The effect of stray magnetic field from the nearby 184" cyclotron is illustrated in Fig. 5, which shows the separation of the two beam components in the target power contours. The peak on the left is from beam ions; the peak on the right is from the neutrals. The ion magnetic drift was in the x-direction (i.e., parallel to the accelerator slots), due to field in the vertical, or y-direction.

Source operational data are plotted in Fig. 6, which shows accelerator voltage, accelerator current and arc power. Since the filaments are emission limited, the relationship of arc power and

accelerator current can only be obtained during beam operation. The backstreaming electron power has a large effect on the plasma density, arc voltage, arc current, and beam current.

The CLPS arc uses emission limited filaments to maximize lifetime. This places a burden on arc and filament power supply controls. The plasma probes had two transients associated with accelerator turnon. The first was an ignorable, fast ( $\leq 1 \mu\text{sec}$ ) transient. The second was a slow (0.1 sec time scale) rise in probe level, due to backstreaming electrons on the filaments. Two techniques were used at LBL to maintain constant accelerator current: 1.) ACCEL ON filament step (i.e., a second step); and 2.) Arc feedback regulation.

The "step" procedure developed for earlier short pulse sources was to reduce the filament power supply at ARC ON. With the CLPS, this first filament step at ARC ON can be to either lower or higher power, depending on whether the filaments have reached thermal equilibrium. Adding a second step to the filament power supply at ACCEL ON is the simplest way to compensate for the backstreaming electron power. The ACCEL ON step is always negative, i.e., to lower filament heater power. The step control should be accessible to the operator, since fine tuning is necessary. The ACCEL ON step sets the asymptotic arc voltage during the beam pulse.

Another procedure for arc compensation is feedback regulation, as used during 80 kV, 30 testing of the 10 x 40 cm prototype.<sup>28</sup> Feedback input could be a plasma probe, accelerator current monitor, or arc power. Feedback worked best if inhibited during the first 50 msec of accelerator operation, to avoid transients associated with accelerator turnon. The feedback response was slowed 50 to 100 msec, to avoid resonance with 60 cycle ripple on the arc and filament power supplies.

Typical OMA spectral data are shown in Fig. 7. Above 100 kV, the OMA deuterium atomic fraction was 80% to 85%. If the arc voltage exceeded 100 Volts, the atomic fraction dropped below 80%, and arc power efficiency also dropped. The minimum atomic fraction observed was 68% at 42 kV, with 10 kW arc.

Water flow calorimetry data indicated that heat loads on the accelerator grids were well below the administrative limit of 1200 Watts per rail during normal source operation. Dissipation of the backstreaming electron heat on the backplate of the arc chamber is critical. The backplate cusps collimate the backstreaming electrons, creating high power densities on the center cusp line. The power absorbed on the center cusp line (which runs in the 48 cm direction) was 32 to 35 kWatts at 120 kV. With the 80 kV accelerator gap, the backplate is a steady state design. The production CLPS backplate is not quite steady state for 120 kV operation. For longer pulses at 120 kV, increased water flow is required for the backplate.

Accelerator grid and electron dump power loads are summarized in TABLE 2. The variation of power load with gas flow, perveance, and gradient grid bias was studied in detail with the 10 x 40 cm source.<sup>7</sup> Operational limits were determined, particularly the dependence of gradient grid and electron dump heat loads on the suppressor grid voltage ratio, as illustrated in Fig. 8. Above 2.8% suppressor bias, the beam heat load on the gradient grid approached the administrative limit of 1200 Watts/rail, and accelerator interrupts became more frequent. Below 1.6% suppressor bias, the backstreaming electron power on the backplate rose precipitously. Vacuum openings and inspection were performed after testing at each suppressor bias. Surface melting was observed on the

copper electron dump (arc backplate) along the center cusp line after 120 kV, 70 Amp, 2 second operation at 1.6% suppressor bias. A suppressor bias of 2.2 to 2.5% is recommended, to maintain a margin of safety.

The end of the test period was used to check a production unit. Source A3/P4-32J1 reached 75 kV, 2 seconds and 84 kV, 1 second in a week of single shift operation, which confirmed that conditioning problems had been solved. Beam properties were very similar to the first source.

## **VII. Discussion**

The CLPS met or exceeded the performance specifications for TFTR in initial testing. Performance has subsequently been confirmed with production sources at TFTR and DIII-D. In 2 second operation, TFTR has reached 105 kV, 71 A hydrogen and 120 kV, 73 A deuterium. This was the first 120 kV operation<sup>9</sup> and injection<sup>10</sup> at TFTR. DIII-D heating beams reached the design goal of 80 kV, 5 seconds in the first hydrogen operation of the 12 x 48 cm, modular focus configuration.<sup>11</sup> Operability and reliability have been excellent, and indications are that filament lifetime will be exceptionally long.

## Acknowledgments

The authors thank W. Lindquist, Lawrence Livermore National Laboratory, for his leadership of this challenging procurement effort. We are pleased to acknowledge the responsiveness of the management and staff of the RCA New Products Division to numerous changes and fixes — especially, F. Hammersand and Ben Adams. LBL staff who made exceptional contributions included D. Yee, mechanical design, R. Kilgore, Controls and Diagnostics; J. Bishop, Electronics; D. Deutscher, Operations; and R. Gray, Mechanical Systems.

This work was supported by the U.S. Department of Energy under Contract No. DE-AC03-76SF00098.

## References

- a) Present address, TRW at Lawrence Livermore National Laboratory,  
Livermore, CA.
- b) Present address, Lawrence Livermore National Laboratory.
- <sup>1</sup>M. C. Vella, O.A. Anderson, K.H. Berkner, C.F. Chan, W.S. Cooper, A.F. Lietzke, J.M. Owren, J.A. Paterson, P.A. Pincosy, R.V. Pyle, and P.D. Weber, Proc. 11th Symp. on Fusion Eng., IEEE Pub. No. CH2251-7, (Austin, TX, November, 1985), p. 149.
- <sup>2</sup>K. H. Berkner, C. F. Burrell, W. S. Cooper, K. W. Ehlers, A. F. Lietzke, H. M. Owren, J. A. Paterson, R. V. Pyle, and J. W. Stearns, Proc. 8th Symp. on Engr. Prob. of Fusion Research, IEEE Pub. No. 79CH1441-5-NPS, (San Francisco CA, November, 1979), p.214.
- <sup>3</sup>M. Akiba, M. Araki, H. Horiike, T. Ito, M. Kawai, M. Kuriyama, S. Kitamura, S. Matsuda, M. Matsuoka, K. Mizuhashi, Y. Oguchi, Y. Ohara, T. Ohga, J. Ohtsuki, Y. Okumura, K. Shibamura, T. Shibata, H. Shirakata, and S. Tanka, Rev. Sci. Instrum. **53**, 1864 (1982).
- <sup>4</sup>A.J.T. Holmes, T.S. Green, and A.F. Newman, Rev. Sci. Instrum. **58**, 1369 (1987).
- <sup>5</sup>H. Altmann, C. Brookes, A. Dines, G. Duesing, H. Falter, A. Goede, R. Haange, R. Hemsworth, B. Nielsen, W. Obert, J. Partridge, P. H. Rebut, V. Simone, D. Stork, And E. Thompson, Proc. 9th Symp. on Engr. Prob. of Fusion Research, IEEE Pub. No. 81CH1715-2-NPS, (Chicago, IL, October, 1981), p. 1338.
- <sup>6</sup>M. Menon, C.C. Tsai, J.H. Whealton, D.E. Schechter, G.C. Barber, S.K. Combs, W.K. Dagenhart, W.L. Gardner, H.H. Haselton, N.S. Ponte, P.M. Ryan, W.L. Stirling and R.E. Wright, Rev. Sci., Instrum. **56**, 242 (1985).



- <sup>7</sup>P.D. Weber, H.M. Owren, J.A. Paterson, P.A. Pincosy, R.V. Pyle, R.P. Wells, and M.C. Vella, *Rev. Sci. Instrum.* **57**, 2714 (1986).
- <sup>8</sup>M.C. Vella, P.A. Pincosy, K. Berkner, C.F. Burrell, K.W. Ehlers, A.F. Lietzke, H.M. Owren, A. Paterson, and R.V. Pyle, International Conference on Plasma Science, IEEE Pub. No. 84CH1958-8 (1984).
- <sup>9</sup>J. Kamperschroer, G.M. Gammel, L.R. Grisham, H.W. Kugel, T.N. Stevenson, A. vonHalle, M.D. Williams, and T.T.C. Jones, *J. Vac. Sci. Tech.* (to be published).
- <sup>10</sup>G.M. Gammel, J. Kamperschroer, L.R. Grisham, H.W. Kugel, R.A. Langely, A.L. Roquemore, M.C. Vella, and M.D. Williams, *Proc. 12th Symp. on Fusion Eng., IEEE*, (Monterey, CA, October, 1987).
- <sup>11</sup>R. Hong, A.P. Colleraine, J.S. Haskovec, D.H. Kellman, J. Kim, A. Nerem, H.C. Phillips, B.W. Sleaford, J.J. Wight, and M.C. Vella, *Proc. 12th Symp. on Fusion Eng., IEEE*, (Monterey, CA, October, 1987).
- <sup>12</sup>I.C. Lutz, C.A. Arthur, G.J. deVries and H.M. Owren, *Proc. 9th Symp. on Engr. Prob. of Fusion Research*, IEEE Pub. No. 81CH1715-2-NPS, (Chicago, IL, October, 1981), p. 427.
- <sup>13</sup>C.F. Burrell, W.S. Cooper, R.R. Smith and W.F. Steele, *Rev. Sci. Instrum.* **51**, 1451 (1980).
- <sup>14</sup>J.A. Paterson, G. Koehler, and R.P. Wells, *Proc. 9th Symp. on Engr. Prob. of Fusion Research*, IEEE Pub. No. 81CH1715-2-NPS, (Chicago, IL, October, 1981), p.1666.
- <sup>15</sup>J.A. Paterson, G.W. Koehler, R.P. Wells and L.A. Biagi, *Proc. 8th Symp. on Engr. Prob. of Fusion Research*, IEEE Pub. No. 79CH1441-5-NPS, (San Francisco CA, November, 1979), p.1065.
- <sup>16</sup>M.C. Vella, K.H. Berkner, D.J. Massoletti, H.M. Owren, and J.E. Willis, *J. Vac. Sci. Technol.*, **20**,1208 (1982).

- <sup>17</sup>M.C. Vella, K.W. Ehlers, D. Kippenhan, P.A. Pincosy, R.V. Pyle, W.F. DiVergilio, and V.V. Fosnight, J. Vac. Sci. Technol. A, **3**, 1218 (1985).
- <sup>18</sup>H. Goede, W.F. DiVergilio, V. V. Fosnight, M.C. Vella, K.W. Ehlers, D. Kippenhan, P.A. Pincosy, R.V. Pyle, Rev. Sci. Instrum. **57**, 1261 (1986).
- <sup>19</sup>K.H. Berkner, W.S. Cooper, K.W. Ehlers, V.L. Jacobson, H.M. Owren, J.A. Paterson, and R.V. Pyle, Third Joint Varenna-Grenoble International Symposium on Heating in Toroidal Plasma, Grenoble, France (March, 1982).
- <sup>20</sup>J.A. Paterson, C.F. Chan, M.Y. Fong, G.W. Koehler, J.S. Sullivan, R.P. Wells, and D.P. Yee, Proc. 11th Symp. on Fusion Eng., IEEE Pub. No. CH2251-7, (Austin, TX, November, 1985), p. 153.
- <sup>21</sup>R.P. Wells, Proc. 11th Symp. on Fusion Eng., IEEE Pub. No. CH2251-7, (Austin, TX, November, 1985), p. 160.
- <sup>22</sup>K.W. Ehlers, Proc. 7th Symp. on Engr. Prob. of Fusion Research, IEEE Pub. No. 77CH1267-4-NPS (Knoxville, TN, October, 1977), p. 291.
- <sup>23</sup>P.A. Pincosy, K.W. Ehlers, A.F. Lietzke, H.M. Owren, J.A. Paterson, R.V. Pyle and M.C. Vella, Rev. Sci. Instrum. **57**, 2705 (1986).
- <sup>24</sup>The authors are pleased to acknowledge the suggestions of Y. Okumura, who was on an exchange visit from JAERI.
- <sup>25</sup>S. Tanaka, M. Akiba, H. Horike, M. Matsuoka, Y. Ohara, and Y. Okumura, Rev. Sci. Instrum. **57**, 145 (1986).
- <sup>26</sup>Y. Ohara, M. Akiba, H. Horiike, H. Inami, Y. Okumura, and S. Tanaka, J. Appl. Phys. **61**, 1323 (1987).
- <sup>27</sup>B. Adams (private communication).
- <sup>28</sup>C.A. Hauck, M.C. Vella, P.A. Pincosy, M.D. Williams, LBL-PUB-3039 (1984).

TABLE 1. Common Long Pulse Source user configurations.

	<u>TFTR</u>	<u>MFTF-B</u>	<u>Doublet Upgrade</u>
Accelerator Voltage	120 kV	80 kV	80 kV
Aperture	12 x 43 cm <sup>2</sup>	12 x 48 cm <sup>2</sup>	12 x 48 cm <sup>2</sup>
Gas	deuterium hydrogen	deuterium hydrogen	hydrogen
Modular Focus	unfocused	unfocused 10 meter	10 meter
Pulse	2 sec	30 sec	5 sec

TABLE 2. Accelerator grid and electron dump central cusp heat loads during 120 kV operation.

<u>Power</u>	<u>Percent Beam Power</u>	
Source grid	590 - 630 W/rail	0.34 - 0.36%
Gradient grid	620 - 670 W/rail	0.36 - 0.39%
Suppressor grid	390 - 440 W/rail	0.23 - 0.25%
Ground grid	380 - 410 W/rail	0.22 - 0.24%
Electron dump, center cusp	31.7 - 34.9 W/rail	0.36 - 0.41%

## Figure Captions

FIG. 1. Assembly drawing of the CLPS plasma generator and accelerator, 48 cm side view.

FIG. 2. Picture of the filaments used for LBL beam testing: 1a) J1; and 1b) Double hairpin.

FIG. 3. Two second divergence tune at 90 kV. The gradient grid bias was 14%, with gas flows from 14 to 24 Tl/s.

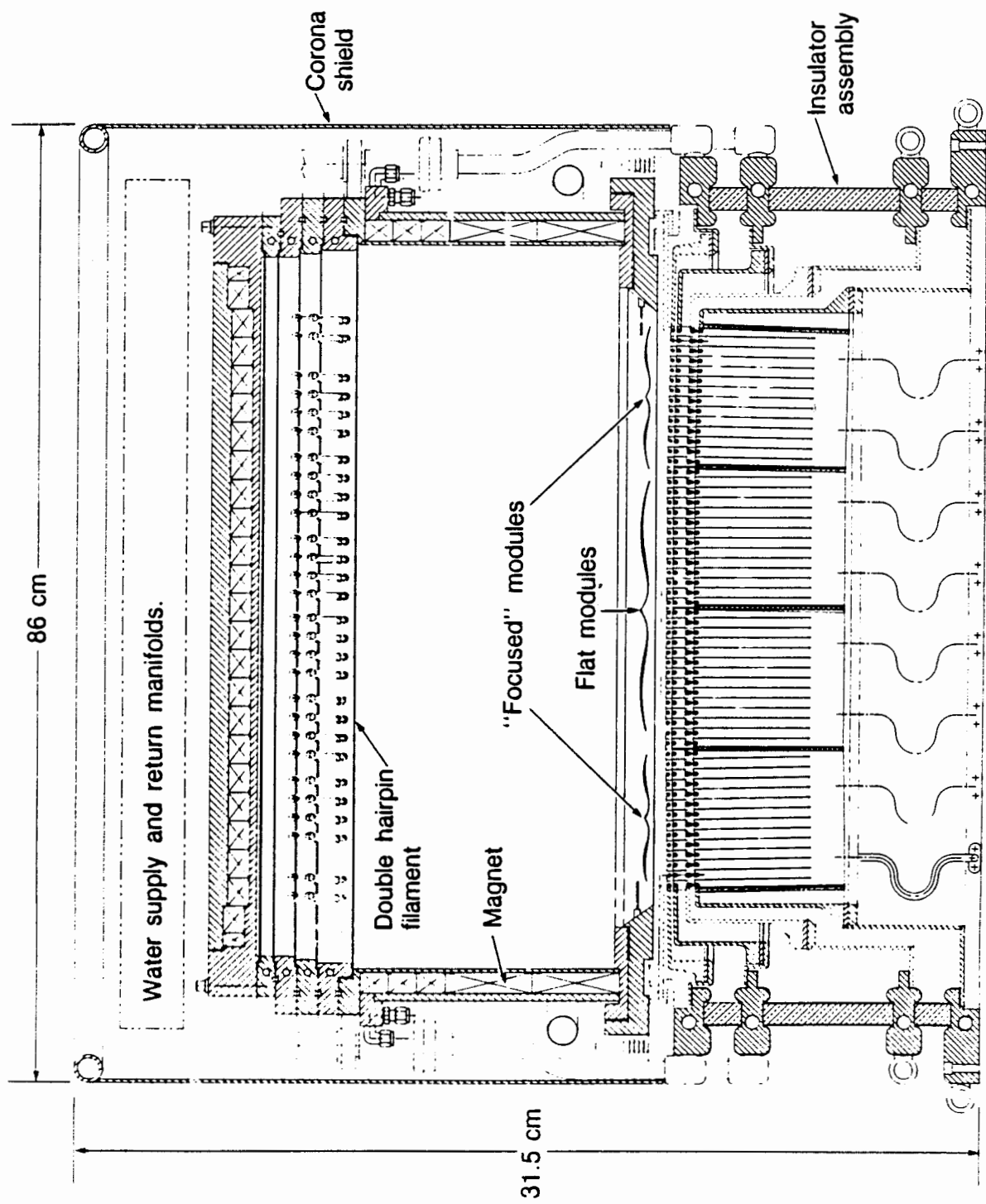
FIG. 4. Selected 120 kV, 2 second divergence data, with gradient grid bias of 12.7%, 13.2% and 14%.

FIG. 5. Active target power density contours for 2 second shot, 120 kV, 71 Amps. The peak on the left is due to beam ions; on the right, beam neutrals. Peak power density was 2300 Watts per cm<sup>2</sup>.

FIG. 6. Operational relationships: 6a) Accelerator current vs accelerator voltage; 6b) Arc power vs accelerator voltage; and 6c) Accelerator current vs arc power.

FIG. 7. Typical OMA spectral data, at 120 kV.

FIG. 8. Variation of absorbed power at 120 kV with suppressor grid bias: 8a) Gradient grid; and 8b) Electron dump center cusp.



XBL 8511-4650 A

Fig. 1

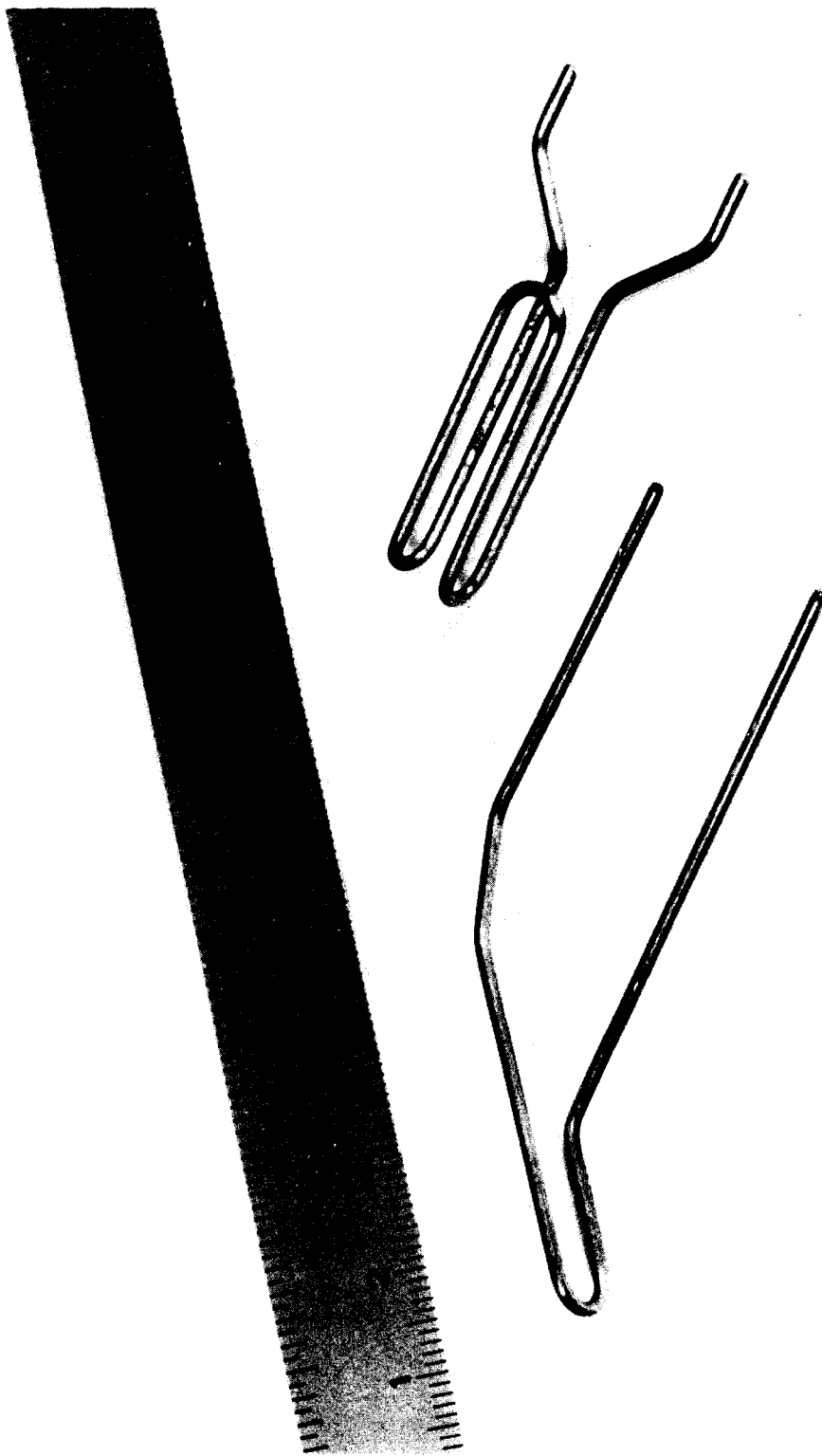
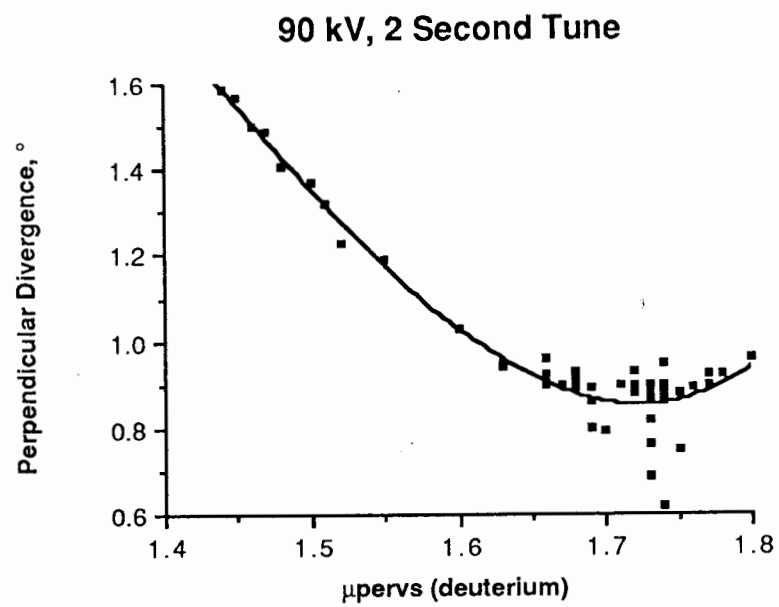


Fig. 2

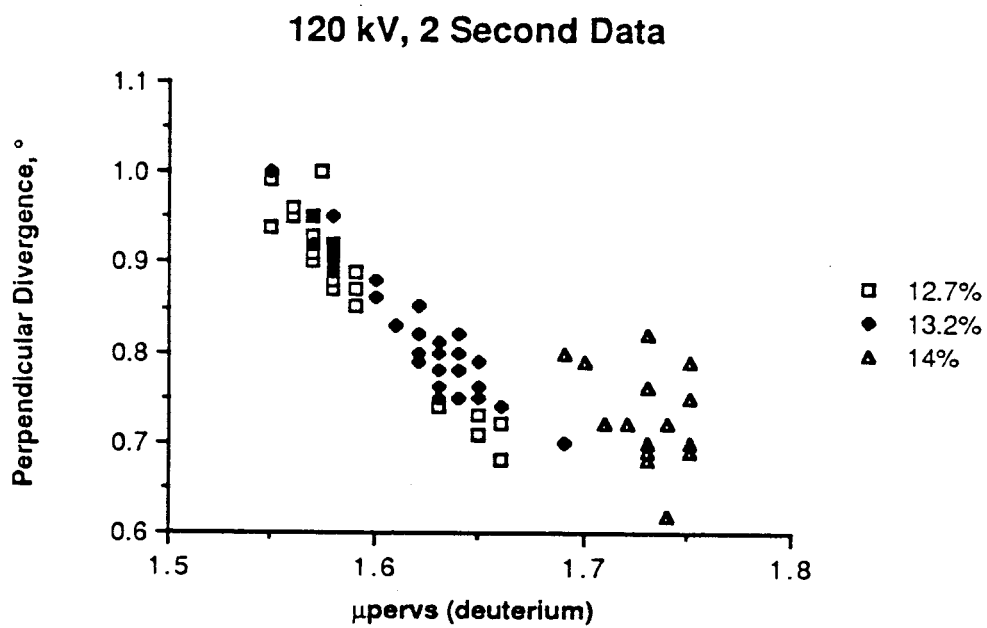
XBB 870-9772



XBL 8711-4795

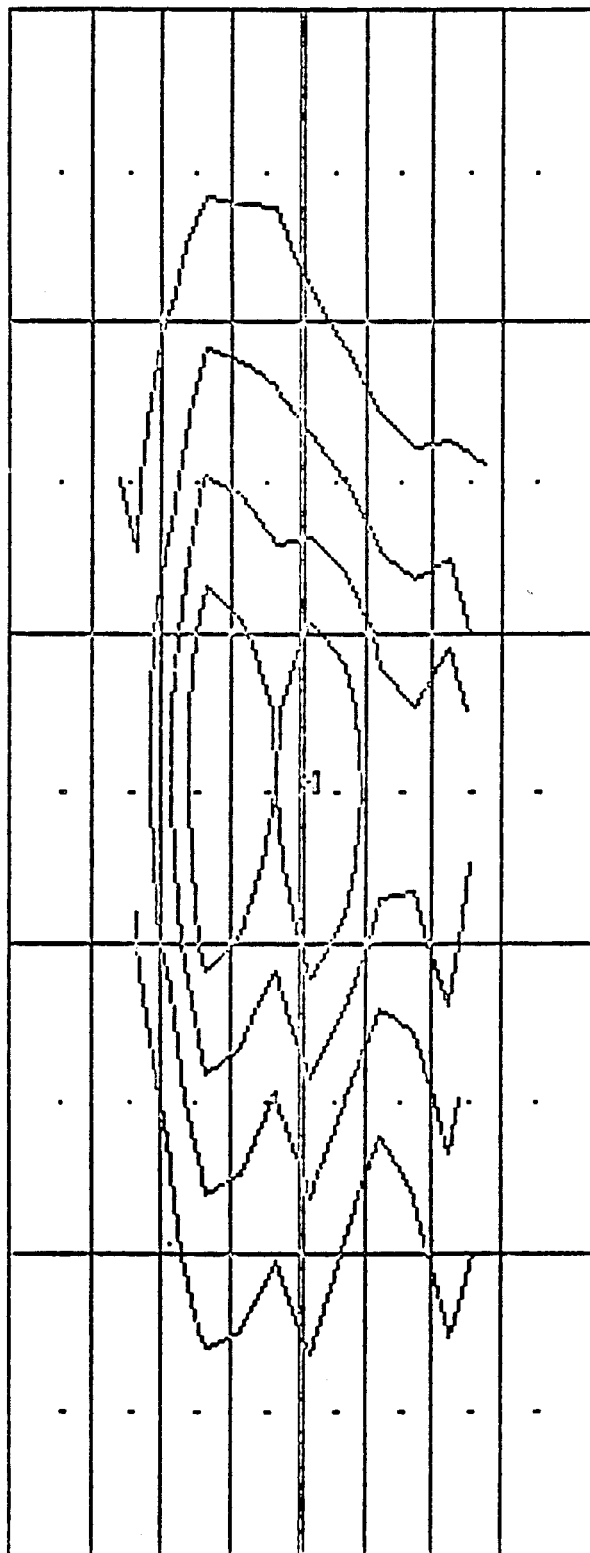
Fig. 3





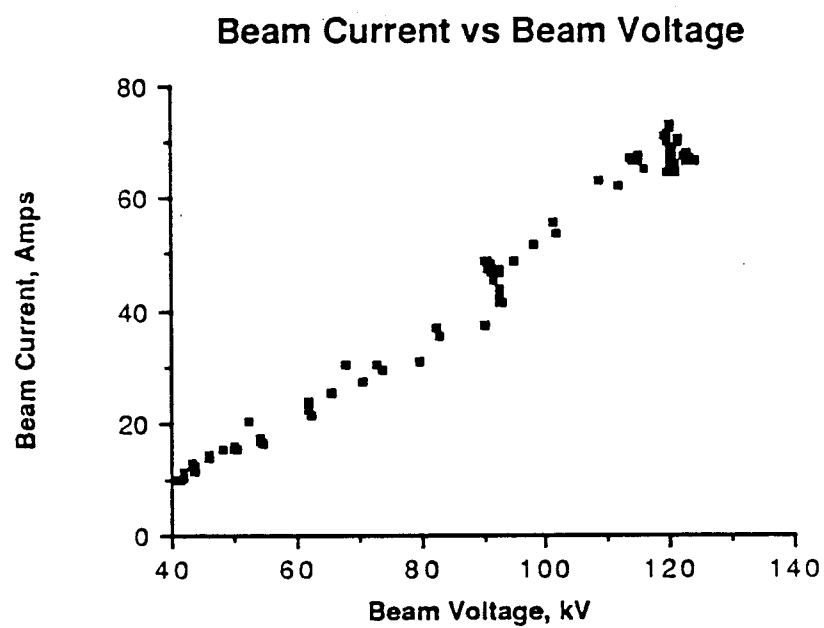
XBL 8711-4796

Fig. 4



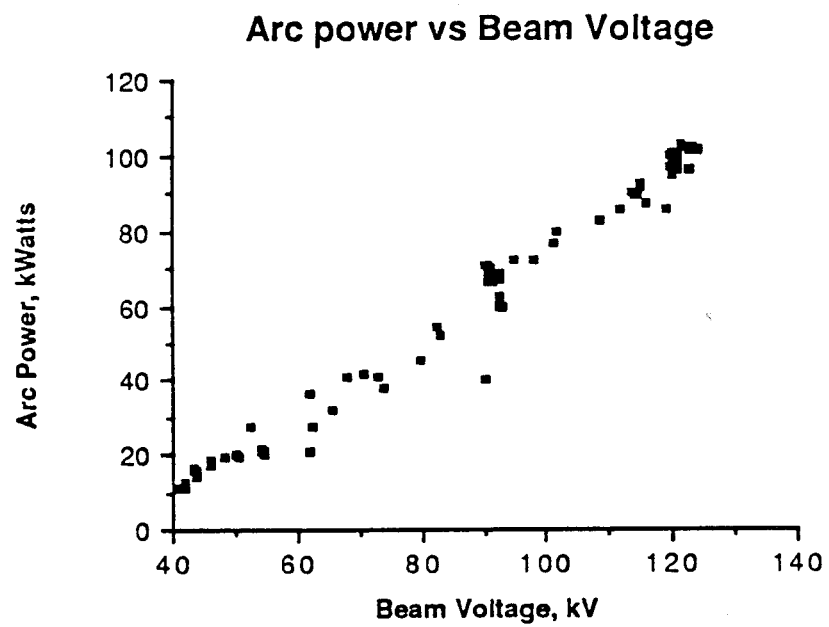
XBL 8711-4777

Fig. 5



XBL 8711-4797

Fig. 6a



XBL 8711-4798

Fig. 6b

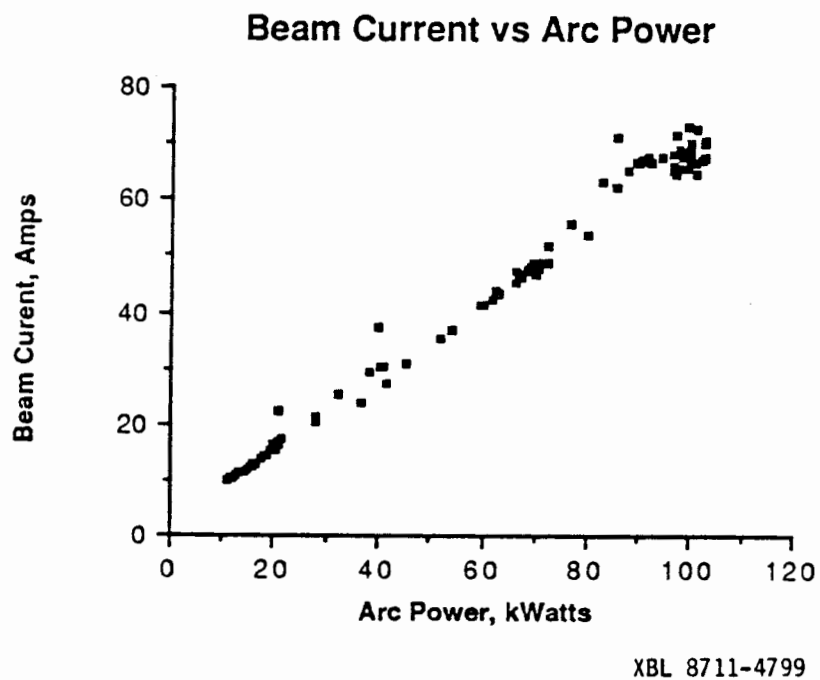
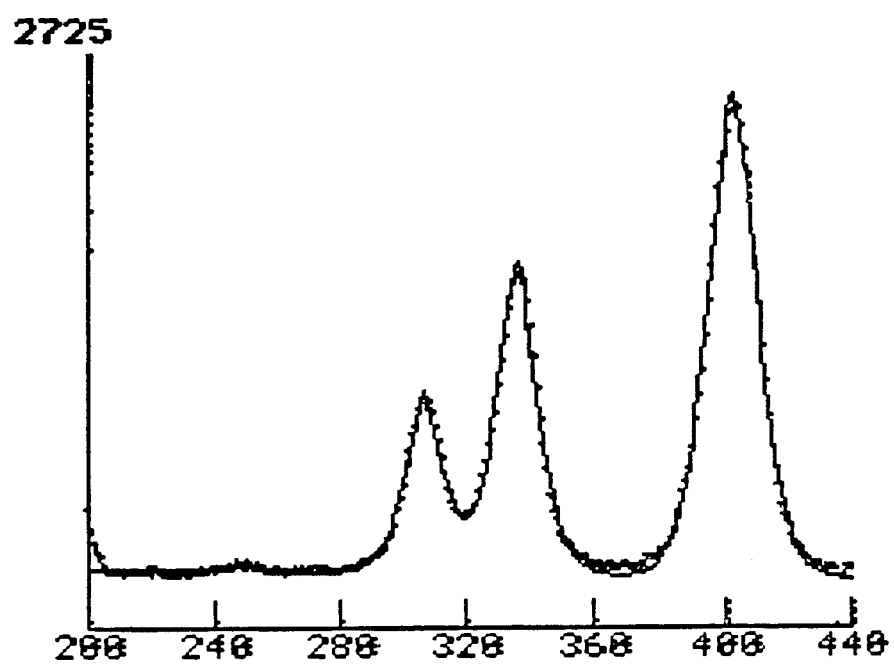
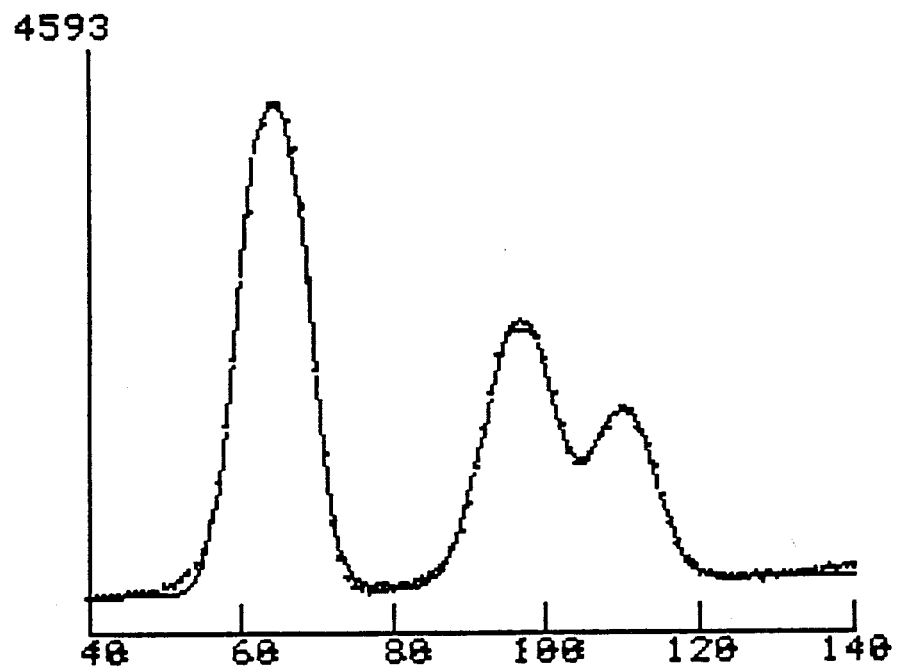


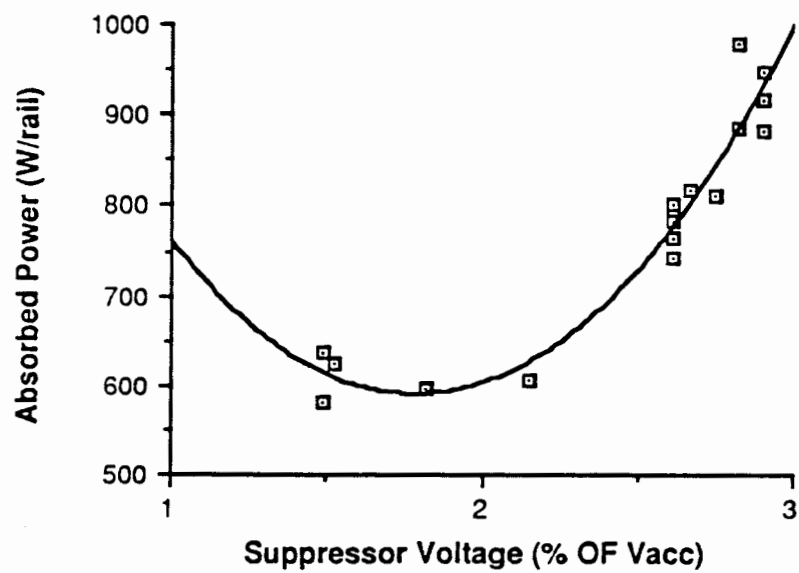
Fig. 6c



XBL 8711-4994

Fig. 7

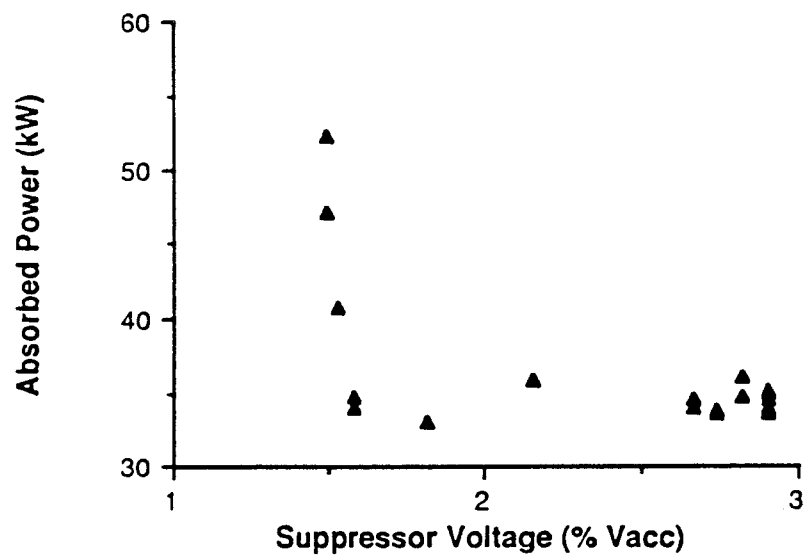
Gradient grid absorbed power vs suppressor bias at 120 kV.



XBL 8711-4800

Fig. 8a

Electron dump center cusp power vs suppressor bias at 120 kV.



XBL 8711-4801

Fig. 8b



